

Phenomenology of a Kinetic Higgs Portal

Anisha^{④, a,b} Lisa Biermann^{④, c} Christoph Englert^{④, d} and Margarete Mühlleitner^{④, a}

^a*Institute for Theoretical Physics, Karlsruhe Institute of Technology, Wolfgang-Gaede-Str. 1, 76131 Karlsruhe, Germany*

^b*Institute for Astroparticle Physics, Karlsruhe Institute of Technology, 76344 Eggenstein-Leopoldshafen, Germany*

^c*PSI Center for Neutron and Muon Sciences, 5232 Villigen PSI, Switzerland*

^d*Department of Physics & Astronomy, University of Manchester, Manchester M13 9PL, United Kingdom*

E-mail: anisha@kit.edu, lisa.biermann@psi.ch,

christoph.englert@manchester.ac.uk, margarete.muehlleitner@kit.edu

ABSTRACT: We explore the phenomenological consequences of non-minimal hidden sector interactions on observable correlations in the Higgs sector, mediated through the \mathbb{Z}_2 -symmetric Higgs portal. Particular attention is given to non-standard momentum dependencies of the hidden sector scalar, which arise naturally in an effective field theory (EFT) framework. We demonstrate that perturbatively reliable constraints can be derived from four-top quark production data and precision measurements of Higgs couplings. These constraints are especially relevant in parameter regions where destructive interference suppresses invisible Higgs decays to light exotic scalars, keeping them within experimentally allowed limits. Finally, we discuss the implications of such hidden sector interactions for the thermal history of the universe. We show that non-standard momentum dependencies open up the Higgs portal to account for the observed dark matter relic abundance whilst evading current direct detection constraints. They can also be probed at the (HL-)LHC and, ultimately, at future lepton colliders such as a FCC-ee.

Contents

1	Introduction	1
2	Effective momentum dependencies	2
3	Phenomenological probes at the LHC and beyond	4
3.1	Direct sensitivity: Invisible Higgs decay searches	4
3.2	Indirect sensitivity	6
3.2.1	Universal on-shell Higgs coupling modifications	6
3.2.2	Processes with Higgs off-shell modifications	9
4	Relevance for early universe physics	11
4.1	The electroweak phase transition	11
4.2	Dark matter relic abundance and direct detection	14
5	Summary and conclusions	15
A	Counting derivative portal interactions at leading order	16

1 Introduction

Searches for physics beyond the Standard Model (BSM) at CERN’s Large Hadron Collider (LHC), albeit unsuccessful so far, give crucial information about the microscopic origin of the electroweak scale. It is widely established that BSM phenomena are required to address critical shortfalls of the Standard Model (SM), whether this concerns the theoretical self-consistency of the SM (through fine-tuning) or agreement with experimental results (e.g. related to dark matter and baryogenesis). On the one hand, in generic approaches to uncover sensitivity to new physics, deviations from the SM are parametrised using effective field theory (EFT), either in the linear (SMEFT) [1] or non-linear (HEFT) versions, cf. e.g., [2–5]. On the other hand, specific and popular extensions of the SM are so-called Higgs portal interactions that seek to marry the dark sector phenomena with the electroweak scale in the SM [6–8]. These leverage one of three renormalisable options to connect the SM to a hidden sector (in addition to kinetic U(1) mixing and mixing with a right-handed sterile neutrino).

The relevance of Higgs portal interactions for the LHC and beyond has been widely researched in the literature (e.g. [9–11]); their appeal for driving a strong first-order phase transition is well-understood [12, 13]. Furthermore, the \mathbb{Z}_2 -symmetric portal model enables a transparent comparison of present and future collider performances across the precision/energy coverage domains that we can expect at such machines (see in particular [14, 15]).

It is conceivable that a hidden sector exhibits a richer phenomenology [16, 17] than parametrised by the minimal Higgs portal. Unless there are sizable non-linearities on the visible side [18], when the hidden sector can be integrated out, it will by construction impart SMEFT-like patterns, even when the hidden sector is highly non-linear. We will see that these interactions are, in some sense, then maximally HEFT-like from the point of view of convergence (see also [19]). Nonetheless, the phenomenology will be dominantly visible through the interactions of the Higgs boson, motivating the language of HEFT to capture these effects transparently, in particular when the hidden degrees of freedom are light [20]. Furthermore, effective portal interactions will enlarge the model’s parameter region, phenomenologically extending beyond the renormalisable correlation expectations.

In this work, we aim to provide a first phenomenological exploration of momentum-dependent, effective portal interactions that extend the traditional portal interactions into the realm of effective field theory (such interactions have been considered more broadly in [21–23]). In particular, we focus on local momentum-dependent interactions in the hidden sector that are communicated to the visible sector in a standard way $\sim \Phi^\dagger \Phi$. Section 2 gives a brief, qualitative motivation on how such interactions can appear in a range of strongly-interacting sectors. In Section 3, we turn to collider probes of such interactions with a particular emphasis on how expected SM correlation patterns are affected by the virtual presence of such physics. This will single out four top production events as motivated candidates to investigate BSM physics more broadly, extending the results of [24] into the region of a light propagating dark sector scalar. The presence of non-minimal interactions can also open up a tuned parameter region where invisible Higgs decays remain in agreement with current Higgs physics constraints. Whilst we do not attempt to provide a dynamic explanation of how such cancellations can occur, we show that our indirect findings are robust in this parameter region. Finally, in Section 4, we clarify how the presence of such interactions can induce or modify a first-order phase transition in the early universe before concluding in Sec. 5.

2 Effective momentum dependencies

As a first example of an effective Higgs portal to strong sectors, consider, e.g., a hidden, QCD-like sector below the symmetry-breaking scale. Its phenomenology will be characterised by a set of pseudo-Nambu Goldstone bosons parametrised by a Callen-Coleman-Wess-Zumino field of the coset G/H (taken as a symmetric space for simplicity), $\xi = \exp(i\pi/f)$ [25, 26]. A Higgs portal, coupled to this sector, can then exhibit low-energy effective interactions, Fig. 1,

$$\mathcal{L}^{\text{EFT}} = \mathcal{L}_{\text{SM}} - \Phi^\dagger \Phi \left(\frac{f^2}{4\Lambda_1^2} \text{Tr}[M(\xi + \xi^\dagger)] + \frac{f^2}{4\Lambda_2^2} \text{Tr}(\partial_\mu \xi^\dagger \partial^\mu \xi) + \dots \right), \quad (2.1)$$

where M is an explicit source of symmetry violation (cf. the light quark flavour masses in QCD) compatible with the \mathbb{Z}_2 -odd symmetry assignment of the would-be pion fields except for a possible Wess-Zumino-Witten term [27, 28]. Momentum dependencies of the effective theory below the cut-off Λ_2 are therefore expected to emerge.

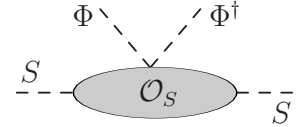


Figure 1. Generic non-minimal \mathbb{Z}_2 -symmetric Higgs portal interactions coupling two emergent scalar S bosons to the SM Higgs doublet Φ via interactions \mathcal{O}_S at the lowest multiplicity order.

This example might seem ad hoc, but it holds more broadly. Turning to interactions more generally, a first look at propagators will be instructive. The (unrenormalised) two-point function of the hidden-sector scalar S can be expressed through a Källén-Lehmann representation [29, 30]

$$\langle 0|T\{S(x)S(0)\}|0\rangle = i \int_0^\infty dq^2 \rho_S(q^2) \int \frac{d^4 p}{(2\pi)^4} \frac{e^{-ip\cdot x}}{p^2 - q^2 + i\epsilon}, \quad (2.2)$$

with the spectral density $\rho_S(q^2)$ of states excited from the vacuum by the quantum field S . The standard single particle-scenario in this parametrisation is obviously recovered through identifying $\rho_S(q^2) \rightarrow \delta(q^2 - m_S^2)|\langle 0|S(0)|q\rangle|^2$ with hidden-sector state excitations characterised by $p_S^2 = m_S^2$. But less canonical representations are possible. For instance, Georgi considered ‘unparticle’ spectral densities in [31]

$$2\pi \theta(q^2)\theta(q^0) \rho_S(q^2) = A_{d_U} \theta(q^2)\theta(q^0) q^{2d_U-4} = \frac{16\pi^{5/2}}{(2\pi)^{2n}} \frac{\Gamma(d_U + 1/2)}{\Gamma(d_U - 1)\Gamma(2d_U)} \theta(q^2)\theta(q^0) (q^2)^{d_U-2}, \quad (2.3)$$

identifying the right-hand side of Eq. (2.3) with the phase space of a non-integral number d_U of massless particles. This is motivated by understanding S as a conformal operator with scaling dimension d_U ; such a theory naturally lends itself to AdS/CFT duality descriptions [32–34]. Entering Eq. (2.3) into Eq. (2.2) leads to a non-local behaviour $\sim x^{-2d_U}$, for $1 \leq d_U < 2$

$$-i \langle 0|T\{S(x)S(0)\}|0\rangle = \frac{A_{d_U}}{2 \sin(d_U \pi)} \int \frac{d^4 p}{(2\pi)^4} \frac{e^{-ip\cdot x}}{(-p^2 - i\epsilon)^{2-d_U}} \xrightarrow{d_U \rightarrow 1} \int \frac{d^4 p}{(2\pi)^4} \frac{e^{-ip\cdot x}}{p^2 + i\epsilon}, \quad (2.4)$$

reducing to a massless propagator for unity operator dimensions.

Fox, Rajaraman, and Shirman [35] proposed a modification $q^2 \rightarrow q^2 - \mu^2$ of Eq. (2.3), introducing an infrared cut-off μ^2 of the original, continuous CFT spectrum to obtain more realistic theories. This also yields the standard scalar propagator for $d_U \rightarrow 1$ and potentially additional poles appearing in the spectrum. The extension to $d_U > 2$ is non-trivial and has been discussed in [34]: The divergent behaviour of the two-point function in this instance requires local subtraction terms, which can quickly dominate the phenomenology as the unparticle spectrum decouples (see also [36]).

This discussion can be extended to $2 \rightarrow 2$ scattering amplitudes that also obey dispersion relations. A generic Higgs portal interaction

$$\mathcal{L} = \mathcal{L}_{\text{SM}} - \eta \Phi^\dagger \Phi \mathcal{O}_S^2, \quad (2.5)$$

with a \mathbb{Z}_2 -odd SM-singlet and scalar operator \mathcal{O}_S can exhibit a highly non-trivial interaction and momentum dependencies. In cases of large anomalous operator dimensions, the above holographic interpretations can be employed to gain qualitative insights. In this case, the three-point function is fixed by conformal symmetry [37], e.g. in the limit $x_{1,2} \rightarrow x_3$ (for the portal $\mathcal{O}_{\text{SM}} = \Phi^\dagger \Phi$)

$$\langle 0|\mathcal{O}_{\text{SM}}(x_1)\mathcal{O}_S(x_2)\mathcal{O}_S(x_3)|0\rangle \sim \frac{1}{|x_{23}|^{2+2d_U}}. \quad (2.6)$$

With subtractions (e.g. to satisfy the Froissart bound [38]), again the interactions are dominated by local terms of an interpolating field S

$$\mathcal{L}^{\text{EFT}} = \mathcal{L}_{\text{SM}} - \Phi^\dagger \Phi \left(\frac{\eta_S}{2} S^2 + \frac{\eta_{KS}}{\Lambda^2} \partial_\mu S \partial^\mu S + \dots \right), \quad (2.7)$$

below the cut-off Λ , very similar to Eq. (2.1), upon expanding the latter.

These interaction terms are reminiscent of a HEFT-like structure in the hidden sector, i.e. the lowest-lying state is described by a singlet that could be coupled in some non-trivial way to a strongly interacting hidden sector below the symmetry-breaking scale. Assuming that the heavy degrees of freedom can communicate with the SM via the portal interaction, a low-energy theory similar to Eq. (2.7) can emerge. It is worthwhile mentioning that the operator in $\sim \eta_{KS}$ is unique in the usual sense of EFT categorisation (see also [21, 22]). We outline this in appendix A. Throughout, we will assume an unbroken \mathbb{Z}_2 symmetry; S does not obtain a vacuum expectation value v_S at zero temperature.

In the following, we will consider Eq. (2.7) as a motivated extension of the standard Higgs portal $\sim \eta_S$. Phenomenologically, this has interesting implications in its own right. Firstly, the portal interactions contribute coherently; $m_S < m_H/2$ can be accessed without directly violating existing Higgs signal strength and hidden Higgs decay measurements. Secondly, the momentum dependencies lead to a non-decoupling behaviour of the extra scalar that sources additional momentum dependencies in the visible sector through radiative corrections. This, of course, does not occur in renormalisable scenarios and can lead to a modification of Higgs-propagation sensitive observables in addition to characteristic Higgs coupling modifications for $m_S > m_H/2$. Thirdly, the momentum dependence translates to a non-trivial modification of the effective Higgs potential, affecting both the temperature-independent and temperature-dependent parts along with the Daisy corrections in the thermal Higgs potential. These terms are known to be relevant near the critical temperature; therefore, the interactions of Eq. (2.7) could have a significant impact on the thermal history of the electroweak scale in the universe, with correlated effects potentially accessible at the LHC.

3 Phenomenological probes at the LHC and beyond

3.1 Direct sensitivity: Invisible Higgs decay searches

We first turn to direct sensitivities at the LHC. In contrast to the standard portal (which is of course recovered for $\eta_{KS} = 0$), the prompt decay $H \rightarrow SS$ is modified for $m_H > 2m_S$

$$\Gamma(H \rightarrow SS) = \frac{1}{32\pi} \sqrt{1 - \frac{4m_S^2}{m_H^2}} \frac{v^2}{m_H} \left(\eta_S + \eta_{KS} \frac{2m_S^2 - m_H^2}{\Lambda^2} \right)^2. \quad (3.1)$$

This singles out a new parameter region for which the invisible Higgs decay width, when $m_H > 2m_S$, is parametrically suppressed for

$$\eta_S \approx \eta_{KS} \frac{m_H^2 - 2m_S^2}{\Lambda^2}. \quad (3.2)$$

When the standard Higgs portal is open for $m_S \simeq 0$, perturbative (if so tuned) choices of the kinetic portal couplings can remove the Higgs signal constraints from a sizeable invisible decay width for perturbative couplings of the standard portal coupling ($m_H = 0.125$ TeV, $m_S \simeq 0$)

$$\eta_S \approx 0.016 \eta_{KS} \left(\frac{\Lambda}{\text{TeV}} \right)^{-2}. \quad (3.3)$$

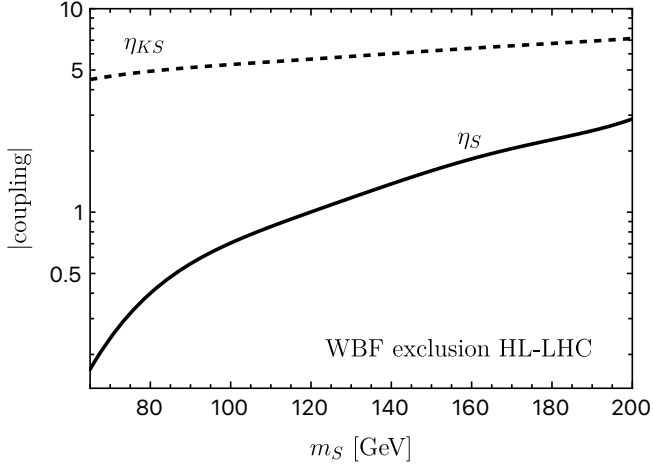


Figure 2. Constraints from a representative invisible Higgs search at ATLAS [47] projected to the HL-LHC phase for off-shell production $m_S > m_H/2$. These direct search constraints on η_{KS} (assuming $\Lambda = 1$ TeV) start to probe the perturbativity limit of the model for $m_S \gtrsim 200$ GeV.

This can be contrasted with unitarity constraints from considering elastic SH scattering using the standard techniques of partial wave projection (see e.g. [39, 40]). Perturbative unitarity of $HS \rightarrow HS$ up to the cut-off $\Lambda \sim \text{TeV}$ at leading order can be achieved for choices $|\eta_{KS}|/\Lambda^2 \lesssim 7/\text{TeV}^2$ relatively independent of the choice of m_S where it can be expected to leave phenomenological footprints at the LHC (we will consider $m_S < 200$ GeV, see below). An invisible branching ratio can therefore be avoided for $\eta_S \sim 1$ for η_{KS} close to the perturbativity limit.

When viewed as a generic, η_S -uncorrelated coupling, measurements from invisible Higgs searches impose constraints on the parameter space. Firstly, combined fits to the observed Higgs signal strengths are relevant measurements for this region, see, e.g. [41]. Furthermore, searches for invisible Higgs decays from jet or Z -associated Higgs production [42–45] as well as weak boson fusion (WBF) production [46] provide direct handles on an invisible Higgs decay. WBF typically provides the stronger constraints, and we will focus on this channel in the comparison of sensitivity based on [47], setting an upper limit of 10.7% on the invisible Higgs branching ratio. This limit is comparable to the constraints from a direct fit to on-shell Higgs signal strengths. However, these direct experimental signatures can also be extended to the $m_H < 2m_S$ regime where the extra scalars can be produced through an off-shell Higgs boson [14, 15]. Reproducing the limits of Ref. [47] and rescaling them with the root of the luminosity, the expected exclusion at the HL-LHC is compared for η_S, η_{KS} (assuming $\Lambda = 1$ TeV) in Fig. 2. As can be seen, the expected exclusion for the kinetic portal begins to lose perturbative sensitivity around 200 GeV. In the following, we will therefore consider $m_S \lesssim 200$ GeV and we will assume $\Lambda = 1$ TeV for definiteness. We will revisit the constraints on the invisible decay width below, comparing directly to the indirect constraints that can be obtained in this model at the LHC.

3.2 Indirect sensitivity

The interactions of Eq. (2.7) modify the Higgs boson propagation, creating HEFT-like interactions, built from the SMEFT-invariant $\Phi^\dagger \Phi$. These interactions are typically moved to other sectors when considering the ‘Warsaw’ basis [1]; such an approach is not economical in this case. Keeping the effects explicit in the Higgs boson two-point function isolates the phenomenological discovery potential more directly. Interactions will

- 1.) modify visible sector Higgs boson couplings uniformly through wave function renormalisation effects in the on-shell scheme (or equivalently BSM contributions to LSZ factors) [48, 49],
- 2.) modify the off-shell behaviour of Higgs propagation
- 3.) introduce new contributions to multi-Higgs vertex functions, including the effective potential.

There are three relevant processes to consider when examining the second point. Firstly, the tree-level electroweak contribution to four top quark production (see, e.g., [50–55]) receives about a 20% electroweak correction. The total next-to-leading (NLO) radiative corrections are sizeable [56], turning four top final states into sensitive BSM tools for discovery, especially when considering Higgs propagator modifications [24]. Secondly, Z boson pair production via $gg \rightarrow ZZ$ has non-decoupling Higgs contributions due to unitarity [57, 58]. Modifications of Higgs boson propagation are therefore a priori relevant. However, the couplings discussed here source oblique Higgs effects that will link vertex and propagator corrections in broken electroweak phases as observed in [24]. We will find that the qualitative EFT results will generalise to the full propagation of light exotic scalars (see below). Thirdly, Higgs pair production is sensitive to the interplay of Higgs two- and three-point interactions. The dominant gluon fusion production mode will therefore probe the full array of BSM modifications: momentum-dependent vertex and propagator corrections as well as coupling modifications [59–61].

3.2.1 Universal on-shell Higgs coupling modifications

The interactions considered in this work primarily affect the physical Higgs fluctuations in the vicinity of the vacuum. In this sense, the interactions $\sim \eta_S, \eta_{KS}$ induce a maximally HEFT-like pattern of SMEFT. In particular, the derivative interactions $\sim \eta_{KS}$ induce new operator structures in the Higgs boson two-point function that are parametrised by the HEFT operator $\sim a_{\square \square} \square H \square H$ [62, 63] that appears in the renormalised Higgs two-point vertex function

$$i\widehat{\Gamma}_{HH}(p^2) = (p^2 - m_H^2) + \Sigma_{HH}^{\text{Loop}}(p^2) + (\delta Z_H(p^2 - m_H^2) - \delta m_H^2) + \frac{2a_{\square \square}}{v^2} p^4. \quad (3.4)$$

(The inverse of this, expanded to a given order in perturbation theory, gives the propagator.) It is, therefore, convenient to exploit the HEFT \supset SMEFT relation and perform the renormalisation programme within the HEFT (see, e.g., [63, 64]). This enables us to go beyond a dimension-six truncation of the interactions directly when computing amplitudes. This is relevant because we consider comparably light BSM spectra and the singularity structure sourced by virtual hidden

sector scalars, which sources SMEFT operators of higher dimension than six.¹ More concretely the finite part of $a_{\square\square}$ in the $\overline{\text{MS}}$ scheme is

$$a_{\square\square}^{\overline{\text{MS}},\text{fin.}} = \frac{\eta_{KS}^2 v^4}{64\pi^2 \Lambda^4} B_0^{\text{fin.}}(p^2, m_S^2, m_S^2), \quad (3.5)$$

where $B_0^{\text{fin.}}$ is the renormalised Passarino-Veltman [65] two-point function. The HEFT parameter is promoted to a form factor, which will generalise to higher-leg HEFT parameters as a function of the relevant Lorentz-scalar quantities. It is instructive to consider the expansion for heavy scalars in the limit $m_S \gg p^2$, which yields

$$a_{\square\square}^{\overline{\text{MS}},\text{fin.}}(\mu^2) = \frac{\eta_{KS}^2 v^4}{64\pi^2 \Lambda^4} \log\left(\frac{\mu^2}{m_S^2}\right) + \mathcal{O}\left(\frac{p^2}{m_S^2}\right), \quad (3.6)$$

with the renormalisation scale μ . In this limit, we recover the expected momentum independence, and this result is also consistent with a renormalisation group flow from matching the SM to the full theory at a scale m_S .

We will set the renormalised HEFT coefficients (such as $a_{\square\square}$ and additional coefficients relevant for HH production, see below) to zero, imagining there are no additional sources that lead to a finite contribution to $a_{\square\square}$ (for extraction strategies see the recent [66]). Finite logarithmic corrections will dynamically source these interactions for process-specific scales $p^2 \neq m_H^2$.

Owing to the nature of the portal interactions, all $\mathcal{O}(\eta_{KS}^2)$ radiative corrections to SM quantities are given by BSM contributions to SM renormalisation constants; Goldstone propagation and Goldstone vertex corrections cancel identically for physical processes at this order. We can therefore perform the calculation in Feynman gauge $\xi = 1$ and afterwards decouple the Goldstone sector in unitary gauge $\xi \rightarrow \infty$ for simplicity. This further highlights the physical Higgs properties as the main phenomenological drivers, as expected in HEFT. Carrying out the renormalisation programme (we give details further below), we find universal coupling modifications for fermions f and massive gauge bosons (suppressing the known η_S result, e.g. [59–61], for convenience)²

$$\begin{aligned} \kappa^V = \kappa^f = 1 + \delta\kappa_H = \\ 1 + \frac{\eta_{KS}^2 v^2}{32\pi^2 \Lambda^4} \left(A_0^{\text{fin.}}(m_S^2) - (m_H^2 - 2m_S^2) B_0^{\text{fin.}}(m_H^2, m_S^2, m_S^2) + \frac{m_H^2 - 2m_S^2}{2} B_0'^{\text{fin.}}(m_H^2, m_S^2, m_S^2) \right), \end{aligned} \quad (3.7)$$

again in terms of the real and renormalised parts of the standard Passarino-Veltman [65] one-loop scalar integrals where A_0, B_0, B_0' (and the derivative of the B_0 function indicated by the prime). We show the sensitivity from projected single Higgs observations (the relative cross section change $\delta\sigma/\sigma$ due to universal coupling modifications) in Fig. 3 for two mass scenarios alongside scale variations in relation to changes of μ . As can be seen, the precision that becomes available at the HL-LHC for single Higgs observables greatly improves over the off-shell suppression of direct production in Fig. 2. When S is light and is characterised such that $H \rightarrow SS$ is suppressed through destructive

¹We choose the on-shell renormalisation scheme for fields and masses and the $\overline{\text{MS}}$ scheme for the additional renormalisation constants.

²We perform calculations in this work with **FeynArts**/**FormCalc**/**LoopTools** [74–80].

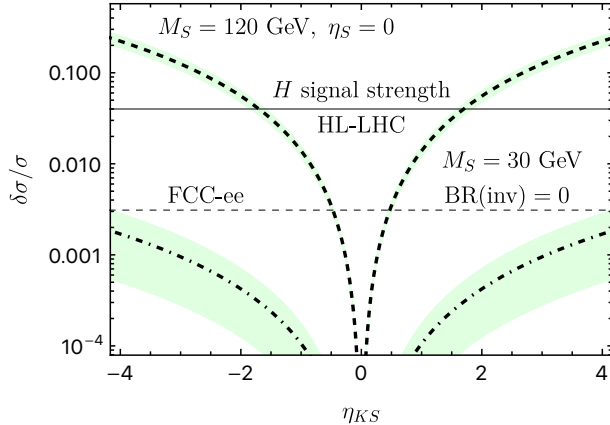


Figure 3. Relative Higgs cross section constraints $\delta\sigma/\sigma$ understood as universal Higgs coupling corrections for different colliders and the model discussed in the text. We show $M_S = 30$ GeV for parameter choices that remove invisible branching ratio constraints (dot-dashed) through a choice of η_S . Also shown is $M_S = 120$ GeV for $\eta_S = 0$ (dashed). The green bands represent the scale uncertainty, which is obtained from varying the renormalisation scale in $\mu \in [0.5m_H, 2m_H]$ for a central choice $\mu = m_H$. Throughout, we choose $\Lambda = 1$ TeV. An optimistic target for the HL-LHC is a 2% determination of universally rescaled SM Higgs couplings [67], which can be improved by a 0.31% measurement of Higgs strahlung [68] at a future Higgs machine (here represented by FCC-ee). Other concepts such as the ILC [69], CLIC [70], CEPC [71], or LCF [72, 73] can obtain quantitatively similar constraints.

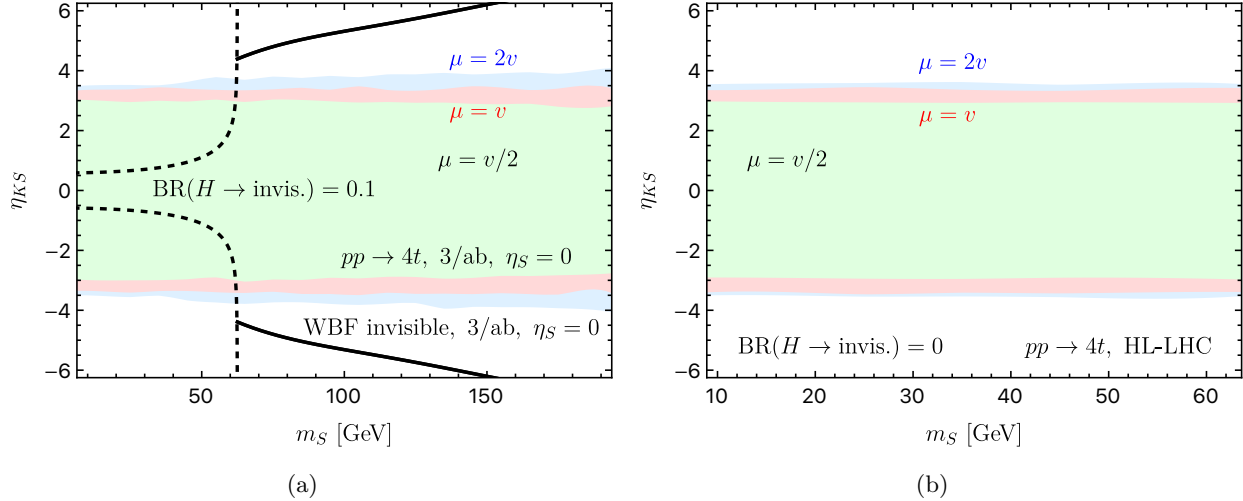


Figure 4. Constraints from four top quark production on the kinetic Higgs portal with $\Lambda = 1$ TeV. In (a), we also show constraints from invisible Higgs constraints imposed by 125 GeV Higgs boson signal strength measurements for $\eta_S = 0$ (black, dashed). These are extended by WBF constraints in the off-shell regime (black solid). (b) shows the constraints on η_{KS} when $\eta_S = \eta_S(\eta_{KS})$ is chosen to remove the invisible Higgs decay according to Eq. (3.1). The different coloured bands correspond to the allowed ranges for different choices of the renormalisation scale μ .

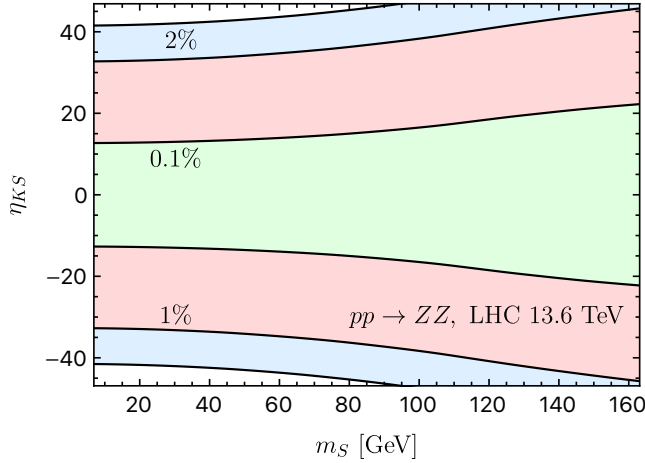


Figure 5. Cross section deviations of $gg \rightarrow ZZ$ from the SM expectation through its dependence on the modified Higgs propagator, for $\eta_S = 0$.

interference, the Higgs coupling modification will fall below the HL-LHC sensitivity threshold. Here, a future e^+e^- Higgs factory could partly regain sensitivity and would efficiently constrain the kinetic portal for heavier states in parallel.

3.2.2 Processes with Higgs off-shell modifications

We now turn to constraining the momentum dependence imparted on the physical Higgs boson's propagation in four top quark, ZZ , and HH production. Firstly, we consider $t\bar{t}t\bar{t}$, which has recently been observed by ATLAS [81] and CMS [82], surpassing their midterm sensitivity extrapolations. It can be expected that the HL-LHC will further improve its sensitivity to this channel, eventually being able to set relatively tight constraints on new physics [83]. Similar to on-shell Higgs production, we renormalise the $t\bar{t} \rightarrow H \rightarrow t\bar{t}$ amplitude. As mentioned above, we can decouple the Goldstone boson contributions so that the off-shell $t\bar{t} \rightarrow t\bar{t}$ amplitudes can be interfaced with `MadGraph_aMC@NLO` [84]. The result for the HL-LHC³, including its sensitivity to scale variations, is shown in Fig. 4 for the four-top production extrapolation to the HL-LHC of [83]. Here we also revisit the combined Higgs signal strength constraints and direct WBF constraints detailed in Sec. 3.1. Indeed, four top quark production is sensitive enough to constrain the parameter space of the kinetic Higgs portal efficiently. This sensitivity, however, is relatively insensitive to the mass scale of the propagating scalar S , which becomes apparent from the comparison of Figs. 4(a) and 4(b).

Next, we consider ZZ production.⁴ Similar to the $t\bar{t} \rightarrow t\bar{t}$ amplitudes the $t\bar{t} \rightarrow ZZ$ amplitude can be renormalised. The universal character of the Higgs portal guarantees a relation between the renormalisation constants⁵

$$-\delta Z_H|_{\text{div}} = \frac{\delta m_W^2}{m_W^2}|_{\text{div}} = \frac{\delta m_t}{m_t}|_{\text{div}} = -\frac{3\eta_{KS}^2}{16\pi^2} \frac{m_S^2}{\Lambda^2} \frac{v^2}{\Lambda^2}, \quad (3.8)$$

³Throughout this paper, we consider 13.6 TeV collisions for our HL-LHC projections.

⁴Both ZZ and HH results have been obtained with `vbfnl` [85].

⁵Electroweak one-loop renormalisation techniques have been reviewed extensively in [86, 87].

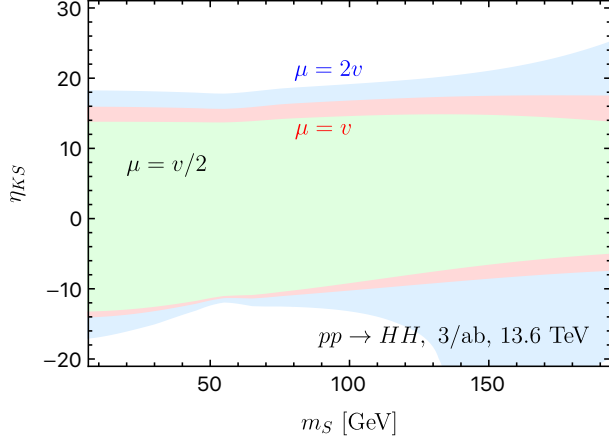


Figure 6. Higgs pair production constraints from ATLAS and CMS projections [90] as described in the text. Also shown is the impact of a scale variation $\mu \in [0.5, 2]v$ for a central scale choice $\mu = v$. We choose $\eta_S = 0$ for illustration.

(again for $\eta_S = 0$ and suppressing the poles in dimensional regularisation $d = 4 - 2\epsilon$) where the renormalisation constants $\delta m_W^2, \delta m_t$ are understood as terms $\sim \Lambda^{-4}$. In particular, a renormalisation of the Weinberg angle is not required. We note the divergent contributions to the Higgs mass renormalisation, as well as the HEFT parameter $a_{\square\square}$ for completeness

$$\delta m_H^2|_{\text{div}} = \frac{\eta_{KS}}{16\pi^2} \frac{m_S^4}{\Lambda^2} \left(1 + 3\eta_{KS} \frac{2m_S^2 - m_H^2}{\Lambda^2} \frac{v^2}{m_S^2} \right), \quad (3.9)$$

$$\delta a_{\square\square}|_{\text{div}} = -\frac{\eta_{KS}^2}{64\pi^2} \frac{v^2}{\Lambda^4}. \quad (3.10)$$

As for $t\bar{t} \rightarrow t\bar{t}$ mentioned above, entering these counterterms in the one-loop renormalised amplitude, we obtain a UV-finite result. The $t\bar{t} \rightarrow ZZ$ amplitude then extends to the $gg \rightarrow H \rightarrow ZZ$ amplitude. The $gg \rightarrow ZZ$ amplitude through fermionic box contributions remains SM-like. This way, the $gg \rightarrow ZZ$ [57, 58, 88] can be generalised to the portal scenario including the virtual S contributions via the $t\bar{t} \rightarrow H \rightarrow ZZ$ subamplitude. As the Higgs contribution is relatively small and given the relation of broken and unbroken phase detailed in [24], the overall corrections are minor, and not large enough to set competitive constraints, see Fig. 5.

Finally, we turn to Higgs pair production. The renormalisation programme has been described in detail in [64]. We treat the tadpole contributions in the parameter-renormalised scheme [87], which requires their inclusion in the renormalisation of the Higgs three-point vertex function (they also contribute to the Goldstone 2-point function). The momentum dependence sourced by the virtual S contributions will renormalise a range of chiral dimension-two and four operators on the HEFT side [89]. Without repeating details here, this requires the renormalisation of the trilinear Higgs coupling κ_3 as well as the HEFT parameters $a_{dd\square}, a_{Hdd}, a_{H\square\square}$ in the basis of [63]. Again, we choose these couplings to vanish at a given renormalisation scale (for measurement strategies of this input data, we refer the reader to [66] once more).

In terms of expected limits, ATLAS and CMS have very recently [90] updated their HL-LHC

projections across a range of motivated double Higgs final states, setting limits on modifications of the Higgs trilinear couplings within $[-26\%, +29\%]$ at 68% confidence level. This interval can be mapped onto a cross section constraint using the cross section interpolation of the Higgs Working Group and [91, 92], and we interpret this cross section constraint $-25\% \lesssim 1 - \sigma/\sigma_{\text{SM}} \lesssim 23\%$ onto the parameter space of the model considered here. The result is shown in Fig. 6. In comparison to the other channels discussed so far, Higgs pair production does not provide competitive constraints and shows a larger vulnerability to scale uncertainties. This is due to the increased relevance of logarithms related to the renormalisation of the multi-Higgs vertex functions (see, e.g., [63, 64]).

4 Relevance for early universe physics

4.1 The electroweak phase transition

The cosmological relevance of the Higgs portal in its standard form $\sim \eta_S$ has been studied extensively in the literature [12, 93–97], in particular with regard to its ability to trigger a first-order phase transition in the early universe. These analyses showed that for a strong-first order phase transition (SFOEWPT) in the vanilla portal scenario, a sizeable η_S of $\mathcal{O}(1)$ is necessary. This directly pits the SFOEWPT against invisible decay widths (and correlated visible channel signal strength constraints) for $m_S < m_H/2$ as well as universal loop-induced coupling modifications for heavier portal scalars, typically leading to large tension. In both regions, the additional freedom of η_{KS} , however, can be exploited to relax experimental constraints.

To quantify the phenomenological outcome, we employ a comprehensive scan over the standard portal scenario $\sim \eta_S$ ($\eta_{KS} = 0$) using `BSMPTv3` [98] to identify a viable SFOEWPT region. We then reevaluate the phenomenology in the light of the η_{KS} discussion above to see if consistent η_{KS} choices are possible to remove the tension with other measurements. We will return to the possibility of driving the phase transition through η_{KS} further below. For definiteness, we will understand the ‘strength’ of the phase transition as

$$\xi_p = \frac{v(T_p)}{T_p}, \quad (4.1)$$

where $v(T_p)$ denotes the Higgs vacuum expectation value at the percolation temperature T_p . A strong first-order phase transition requires $\xi_p > 1$ (additional details can be found in [98]). Depending on the parameter choices, we find first-order transitions with one or two steps between phases with typically non-zero v_S , while $v_S = 0$ at zero temperature. The strength ξ_p is evaluated for the step in which the Higgs vacuum v changes from zero to a non-zero value at the corresponding percolation temperature.

We start with the parameter region $m_S < m_H/2$. We find in our scan that parameter choices for η_{KS} that suppress invisible Higgs decays violate the unitarity constraints for our benchmark choice of $\Lambda = 1$ TeV. Hence, a viable SFOEWPT due to η_S cannot be compensated with perturbative η_{KS} choices. Lower scales are imaginable, but these would lead inadvertently to strong coupling effects dialled into the visible sector as well.

Turning to $m_S > m_H/2$ in our scan, a successful SFOEWPT driven by η_S leads to universal Higgs coupling modifications at $\mathcal{O}(\eta_S^2)$ that are large enough to constrain this parameter region at present already. Approaching the HL-LHC phase, the entire parameter region probed in our scan can

be ruled out. Again, cancellations at one-loop are possible given the parametric freedom of η_{KS} . And for our $\eta_S \neq 0$ scan points, these are within the perturbative range, we find $|\eta_{KS}|/\Lambda^2 \lesssim 6/\text{TeV}^2$ just below the perturbativity limit quoted above. Through an appropriate choice of η_{KS} , cancelling the impact of $\eta_S \neq 0$, the single Higgs observables will not be sensitive at the one-loop level, highlighting double Higgs production as the remaining potentially sensitive collider probe of this parameter region. For such choices, the double Higgs production cross section modifications are, however, below 1%, compared to the SM expectation; the bulk of the (ad hoc) single Higgs phenomenology cancellations carry over to multi-Higgs final states. These cross section modifications are too small to be observable at the LHC. Therefore, within the scope of our analysis, we are forced to conclude that whilst a η_S -driven SFOEWPT can be obtained in the kinetic portal scenario, this seems only possible through a delicate balance of coupling choices close to the strong coupling limit that leave no additional collider sensitivity otherwise — a theoretically unappealing avenue.

Next, we investigate how η_{KS} reshapes phase transitions and whether there is a possibility to realise an SFOEWPT through a *combination* of η_{KS}, η_S effects. Including the non-trivial kinematic dependence η_{KS} , the one-loop effective potential⁶ arising from S exchange is modified as

$$V_S^{(1)}(\phi_C) = i \sum_{n=1}^{\infty} \int \frac{d^4 q}{(2\pi)^4} \frac{1}{2n} \left[\frac{(\eta_S + 2\eta_{KS} q^2/\Lambda^2) \phi_C^2}{q^2 - m_S^2 + i\epsilon} \right]^n, \quad (4.2)$$

upon summing all 1-particle irreducible S insertions at one-loop (where ϕ_C is the background Higgs field). The calculation can be tackled with standard techniques, e.g. [100], which yields a volume effect

$$V_S^{(1)}(\phi_C) = \alpha^{-4}(\phi_C, \eta_{KS}) V_S^{(1)}(\phi_C, \eta_{KS} = 0), \quad (4.3)$$

with

$$\alpha^2(\phi_C, \eta_{KS}) = 1 - \eta_{KS} \frac{\phi_C^2}{\Lambda^2}. \quad (4.4)$$

Here, $V_S^{(1)}(\phi_C, \eta_{KS} = 0)$ denotes the ‘standard’ portal interaction Coleman-Weinberg potential, which is trivially recovered for $\eta_{KS} = 0$.

The finite temperature $T \neq 0$ contribution can be computed similarly. It is given by

$$\begin{aligned} V_{S,T}^{(1)}(m_S(\phi_C)) &= \frac{1}{\alpha^4} \frac{\alpha^4 T^4}{2\pi^2} J_B \left(\frac{m^2}{\alpha^2 T^2} \right) = \frac{1}{\alpha^4} V_{S,\alpha T}^{(1)}(m_S(\phi_C), \eta_{KS} = 0) \\ &= V_{S,T}^{(1)}(m_S(\phi_C)/\alpha, \eta_{KS} = 0), \end{aligned} \quad (4.5)$$

with the standard bosonic J_B function, see e.g. [100]. Again, this reproduces the standard portal result for vanishing η_{KS} .

Effectively, η_{KS} leads to a change in inertia that exerts itself as an overall modification of energy densities (as it is equivalent to a scale transformation in momentum space), as well as through an effective change in temperature of the thermal bath. When the effective inertia is small, modes $m(\phi_c)$ are easily excited, in a given thermal bath and background field ϕ_C . The temperature that characterises the same free energy of the plasma appears lower compared to the $\alpha = 1$ case.

⁶We refer the reader to Ref. [99] for recent and new insights into the effective potential’s gauge-(in)dependence.

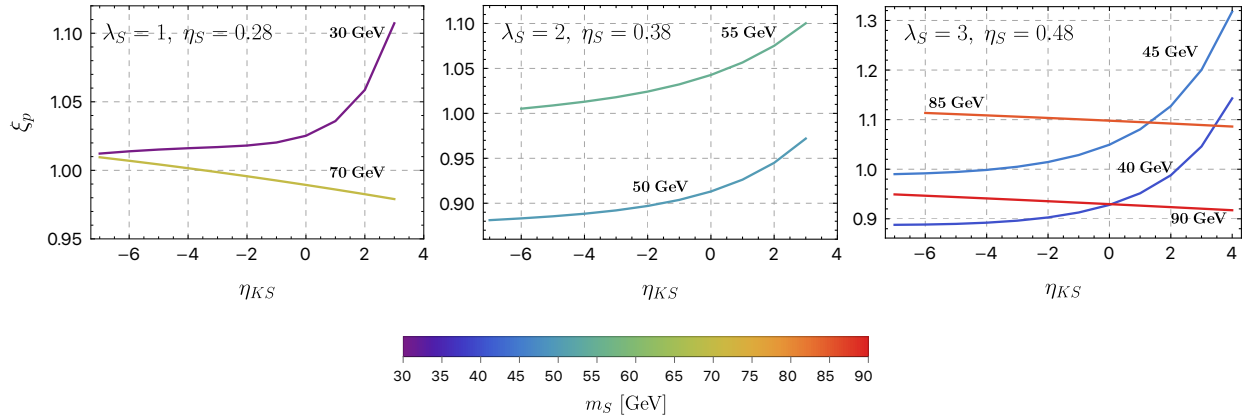


Figure 7. Response of the phase transition strength ξ_p with varying η_{KS} for $\Lambda = 1$ TeV. The plots are shown for three chosen benchmark points, with different values of m_S indicated by the colorbar. The figure panels shows ξ_p : leftmost, for $m_S = 30$ and 70 GeV with $\lambda_S = 1$, $\eta_S = 0.28$; center, $m_S = 50$ and 55 GeV with $\lambda_S = 2$, $\eta_S = 0.38$; rightmost, $m_S = 40, 45, 85, 90$ GeV for $\lambda_S = 3$, $\eta_S = 0.48$. Here, λ_S denotes the quartic S self-coupling $\sim \lambda_S S^4/4!$.

Equivalently, as m^2 breaks classical scale invariance, at finite temperature, the potential can also be understood as an increased effective mass for $\alpha < 1$ at the same temperature T that species $\alpha = 1$ feel.

Additionally, there are thermal mass corrections to the SM scalar bosons that need to be included via the Daisy resummation. In the high-temperature limit, these are

$$\Delta \bar{m}^2 = \frac{\eta_{KS}}{12} \frac{m_S^2(\phi_C)}{\Lambda^2} T^2. \quad (4.6)$$

The scalar S does not receive additional thermal corrections beyond the standard portal interaction $\sim \eta_S$ and its self-coupling that are well-documented in the literature [100].

To explore the parameter space relevant for SFOEWPTs numerically, the above-mentioned modifications to the effective potential are implemented in **BSMPTv3**. We again deploy our previously mentioned **BSMPTv3** scan without imposing collider constraints at this stage. The parameter points with $\xi_p \sim 1$ are then selected to study the impact of an EFT portal coupling, which is varied within its perturbative limit, $|\eta_{KS}| \leq 7$, for $\Lambda = 1$ TeV.

For lighter singlet masses $m_S \leq 55$ GeV, we observe that the phase transition strength increases with increasing η_{KS} , whereas for $m_S > 55$ GeV, it decreases. This behaviour is illustrated in Fig. 7 for three different benchmarks at different singlet masses. We note that the light mass choices, for which $\xi_p > 1$ is achieved via η_{KS} , are not compatible with constraints from the 125 GeV Higgs signal strength measurements due to a large invisible Higgs decay width $H \rightarrow SS$. These parameter choices are also in tension with direct detection experiments (see below). Whilst driving an SFOEWPT does not seem possible within the constraints of the effective model analysed here, we can expect that a realistic theory of a strongly-interacting hidden sector contains more degrees of freedom that can drastically change the conclusions presented here for a single interpolating field.

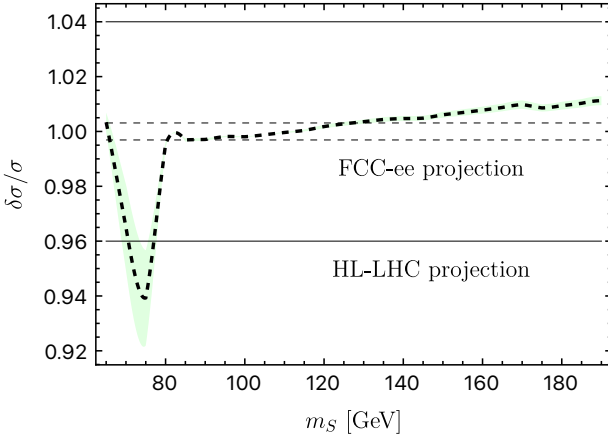


Figure 8. Expected cross section deviation in the kinetic portal model as a function of m_S . η_S, η_{KS} are chosen to reproduce the correct DM relic abundance whilst evading DM direct detection constraints as implemented in `micrOMEGAs` [101]. Further details are given in the main text. Again, we show a scale variation by a factor of two around a central scale choice $\mu = m_H$ as the green-shaded region. The horizontal lines represent the constraints that can be achieved at the respective colliders, cf. Fig. 3.

4.2 Dark matter relic abundance and direct detection

Understanding the \mathbb{Z}_2 -odd scalar as a minimal solution to the WIMP miracle is experimentally challenged. The generic finding of the standard singlet scenario is that the concordance of dark matter relic abundance $\Omega_{\text{DM}} h^2 \simeq 0.12$ and direct detection exclusion leads to a substantial tension. If the hidden sector is less minimal and contains additional fields, this tension can be reduced. Nonetheless, to gauge the compatibility of the discussed scenario with these data, we will assume here that S is indeed stable and the only relevant state for direct detection and relic abundance computations. Similar to extending the parameter space via the kinetic interactions $\sim \eta_{KS}$ into the regime $m_S \leq m_H/2$, we can then also revisit the implications for astrophysics. We employ `micrOMEGAs` [101] to identify regions of the (m_S, η_S, η_{KS}) parameter space where the correct DM relic abundance is reproduced whilst no direct detection constraints can be obtained. In this region $m_S \lesssim m_H/2$, we find that a benchmark choice

$$m_S = 55 \text{ GeV}, \eta_{KS} = -0.3, \eta_S = 0.003, (\text{BR(inv)} = 1.9\%), \quad (4.7)$$

is consistent with experimental observations and can approximate the astrophysical data within 10%. Viewed against our previous discussion of Sec. 4.1, it is clear that this region is not compatible with the simultaneous requirement of an SFOEWPT. The viable region in parameter space for $m_S \lesssim m_H/2$ is small and well-represented by this point. The coupling deviations for this parameter point will also be observable at a future Higgs factory [68]; the invisible branching ratio exceeds the (representative) 0.31% accuracy obtainable for Higgs production at a lepton collider.⁷

Turning to regions $2m_S > m_H$, around the threshold region, much bigger η_{KS} are allowed, reaching $|\eta_{KS}| \simeq 4.5$ around 70 GeV. Relic abundance and direct detection results are reproduced

⁷As part of the renormalisation programme detailed in the previous section, we have checked that the RGE flow does not significantly change the correlation between measurements at the involved different energy scales.

by $\eta_S \simeq 0.04$. Here, the observed cross section modification is detectable. The Higgs cross section modifications in this region are shown in Fig. 8, in comparison to the projected associated Higgs production at a future FCC-ee. (Other lepton colliders discussed in the literature such as the ILC [69], CLIC [70], CEPC [71], or LCF [72, 73] can obtain a quantitatively similar measurement.) The largest deviations we find here are $\sim 5\%$. An increased sensitivity beyond the current extrapolations (see e.g. [83]), could open up additional sensitivity at the HL-LHC. Given that four top production is insensitive to η_S in this range, cf. Fig. 4, these final states can, in principle, add complementary sensitivity during the HL-LHC phase.

5 Summary and conclusions

Non-minimal Higgs sector extensions arise in a multitude of BSM theories. In this work, we have focused on strongly interacting hidden sectors that give rise to non-standard effective modifications of the so-called Higgs portal. The leading effects of such interactions can be motivated from chiral perturbation theory and its large N generalisation via AdS/CFT, and they are kinetic in nature, introducing unique non-standard momentum dependencies at the dimension-six level.

Phenomenologically, such interactions manifest themselves predominantly through modifications of the physical Higgs boson. In this sense, the phenomenology is well-captured in a HEFT approach, albeit communicated to the SM sector in a SMEFT-like fashion. We find that the effects of the kinetic portal extension can be probed in universal Higgs coupling modifications. Due to its indirect sensitivity, this information is insufficient to reveal the momentum-dependent nature of the extension in the presence of standard, renormalisable couplings. The non-decoupling nature of these interactions (below the hidden sector’s intrinsic mass scale, here taken to be $\mathcal{O}(\text{TeV})$), however, highlights other phenomenological arenas for sensitivity, as they can leave sizeable radiative imprints on visible-sector observables. We demonstrate that the dominant sensitivity can be found in four top quark final states, with reduced sensitivity from Higgs pair and Z pair production (in this order). These constraints remain relevant when destructive interference removes sensitivity from Higgs signal strength and invisible decay searches for light exotic scalar masses.

Such non-trivial momentum dependencies can impact the physics of the early Universe.⁸ Especially when the exotic hidden sector scalar is light, the electroweak phase transition can receive significant modifications compared to the SM-expected crossover. Thus, for lighter hidden sector scalars, the strength of the phase transition can be modified to first-order through the η_{KS} coupling. This region is tensioned by Higgs signal strength measurements and invisible Higgs decay searches. For heavier S , η_{KS} has a reduced relevance for driving an SFOEWPT.

Furthermore, the higher-dimensional interactions resurrect the Higgs portal’s ability to act as a viable dark matter candidate, satisfying relic abundance and direct detection constraints. This parameter region can be experimentally explored at the HL-LHC phase through universal Higgs coupling modifications and changes compared to the SM-expected four top phenomenology. A future

⁸They will also affect more broadly astrophysical observations related to strongly interacting dark sectors such as the cusp vs. core anomaly [102], the ‘too big to fail’ problem [103] or the missing-satellites problem [104], e.g. by modifying galaxy core formation and feedback. We leave this for the future; results will crucially depend on the hidden sector dynamics.

Higgs factory, such as the widely-discussed FCC-ee, amongst others, will add further discovery potential through an accurate determination of Higgs couplings.

Acknowledgements

We thank Victor Maura Breick, Max Detering, Suraj Prakash and Tevong You for helpful discussions on matters related to this work. A. and M.M. acknowledge support by the Deutsche Forschungsgemeinschaft (DFG, German Research Foundation) under grant 396021762 - TRR 257. The work of L.B. is supported by the Swiss National Science Foundation (SNSF). C.E. is supported by the STFC under grant ST/X000605/1, and by the Leverhulme Trust under Research Fellowship RF-2024-300\9. C.E. is further supported by the Institute for Particle Physics Phenomenology Associateship Scheme.

A Counting derivative portal interactions at leading order

For derivative operators of class $\phi^4 D^2$ (with $\phi = \Phi, S$) involving a \mathbb{Z}_2 symmetric singlet, an additional invariant structure $\Phi^2 S^2 D^2$ (see Refs. [21, 22]) is possible using the Hilbert series method, in addition to the SMEFT $\Phi^4 D^2$ operators. The following gauge-invariant structures with two derivatives are possible in combination with the gauge-singlet Higgs operator $\Phi^\dagger \Phi$

$$\Phi^\dagger \Phi \partial_\mu S \partial^\mu S, \tag{A.1}$$

$$\partial_\mu (\Phi^\dagger \Phi) S \partial^\mu S, \tag{A.2}$$

$$\square (\Phi^\dagger \Phi) S^2, \tag{A.3}$$

$$\Phi^\dagger \Phi S \square S. \tag{A.4}$$

The last of these, Eq. (A.4) $\sim \square S$, is linked to the equations of motion (EOM) of S and in systematic expansion in the EFT scale, these interactions are removed [1] as these reduce to ϕ^4 (dim-4 portal $\Phi^\dagger \Phi S^2$) and ϕ^6 structures.⁹ We can rewrite Eq. (A.3) using integration by parts (IBP), e.g.

$$\square (\Phi^\dagger \Phi) S^2 \rightarrow \partial_\mu (\Phi^\dagger \Phi) \partial^\mu (S^2) \rightarrow \partial_\mu (\Phi^\dagger \Phi) S \partial^\mu S. \tag{A.5}$$

Similarly, starting from $\partial_\mu (\Phi^\dagger \Phi S \partial^\mu S)$, we have

$$\partial_\mu (\Phi^\dagger \Phi) S \partial^\mu S \rightarrow (\Phi^\dagger \Phi) S \square S + (\Phi^\dagger \Phi) \partial_\mu S \partial^\mu S, \tag{A.6}$$

and thus we can also omit Eq. (A.2). This leaves Eq. (A.1) as the non-redundant structure for the lowest-order momentum deformation of the Higgs portal. Therefore, for the results presented in this work, it is sufficient to consider the interaction (A.1).

References

[1] B. Grzadkowski, M. Iskrzynski, M. Misiak and J. Rosiek, *Dimension-Six Terms in the Standard Model Lagrangian*, *JHEP* **10** (2010) 085, [1008.4884].

⁹As EOMs are not equivalent to redundant field redefinitions, the theories obtained this way are not strictly identical [105]. A complete renormalisation programme of off-shell Green's functions at a given order requires additional care. This has been transparently demonstrated in Ref. [106].

- [2] A. C. Longhitano, *Low-Energy Impact of a Heavy Higgs Boson Sector*, *Nucl. Phys. B* **188** (1981) 118–154.
- [3] F. Feruglio, *The Chiral approach to the electroweak interactions*, *Int. J. Mod. Phys. A* **8** (1993) 4937–4972, [[hep-ph/9301281](#)].
- [4] T. Appelquist and G.-H. Wu, *The Electroweak chiral Lagrangian and new precision measurements*, *Phys. Rev. D* **48** (1993) 3235–3241, [[hep-ph/9304240](#)].
- [5] R. Alonso, M. B. Gavela, L. Merlo, S. Rigolin and J. Yepes, *The Effective Chiral Lagrangian for a Light Dynamical "Higgs Particle"*, *Phys. Lett. B* **722** (2013) 330–335, [[1212.3305](#)].
- [6] T. Binoth and J. J. van der Bij, *Influence of strongly coupled, hidden scalars on Higgs signals*, *Z. Phys. C* **75** (1997) 17–25, [[hep-ph/9608245](#)].
- [7] B. Patt and F. Wilczek, *Higgs-field portal into hidden sectors*, [hep-ph/0605188](#).
- [8] R. M. Schabinger and J. D. Wells, *A Minimal spontaneously broken hidden sector and its impact on Higgs boson physics at the large hadron collider*, *Phys. Rev. D* **72** (2005) 093007, [[hep-ph/0509209](#)].
- [9] V. Barger, P. Langacker, M. McCaskey, M. J. Ramsey-Musolf and G. Shaughnessy, *LHC Phenomenology of an Extended Standard Model with a Real Scalar Singlet*, *Phys. Rev. D* **77** (2008) 035005, [[0706.4311](#)].
- [10] X.-G. He, T. Li, X.-Q. Li, J. Tandean and H.-C. Tsai, *The Simplest Dark-Matter Model, CDMS II Results, and Higgs Detection at LHC*, *Phys. Lett. B* **688** (2010) 332–336, [[0912.4722](#)].
- [11] C. Englert, T. Plehn, D. Zerwas and P. M. Zerwas, *Exploring the Higgs portal*, *Phys. Lett. B* **703** (2011) 298–305, [[1106.3097](#)].
- [12] S. Profumo, M. J. Ramsey-Musolf and G. Shaughnessy, *Singlet Higgs phenomenology and the electroweak phase transition*, *JHEP* **08** (2007) 010, [[0705.2425](#)].
- [13] L. Biermann, M. Mühlleitner and J. Müller, *Electroweak phase transition in a dark sector with CP violation*, *Eur. Phys. J. C* **83** (2023) 439, [[2204.13425](#)].
- [14] M. Ruhdorfer, E. Salvioni and A. Weiler, *A Global View of the Off-Shell Higgs Portal*, *SciPost Phys.* **8** (2020) 027, [[1910.04170](#)].
- [15] C. Englert, J. Jaeckel, M. Spannowsky and P. Stylianou, *Power meets Precision to explore the Symmetric Higgs Portal*, *Phys. Lett. B* **806** (2020) 135526, [[2002.07823](#)].
- [16] C. Gross, O. Lebedev and T. Toma, *Cancellation Mechanism for Dark-Matter–Nucleon Interaction*, *Phys. Rev. Lett.* **119** (2017) 191801, [[1708.02253](#)].
- [17] J. C. Criado, A. Djouadi, M. Perez-Victoria and J. Santiago, *A complete effective field theory for dark matter*, *JHEP* **07** (2021) 081, [[2104.14443](#)].
- [18] I. Brivio, M. B. Gavela, L. Merlo, K. Mimasu, J. M. No, R. del Rey et al., *Non-linear Higgs portal to Dark Matter*, *JHEP* **04** (2016) 141, [[1511.01099](#)].
- [19] A. Helset, A. Martin and M. Trott, *The Geometric Standard Model Effective Field Theory*, *JHEP* **03** (2020) 163, [[2001.01453](#)].
- [20] Anisha, S. Das Bakshi, C. Englert and P. Stylianou, *Higgs boson footprints of hefty ALPs*, *Phys. Rev. D* **108** (2023) 095032, [[2306.11808](#)].
- [21] H. Song, H. Sun and J.-H. Yu, *Complete EFT operator bases for dark matter and weakly-interacting light particle*, *JHEP* **05** (2024) 103, [[2306.05999](#)].

[22] H. Song, H. Sun and J.-H. Yu, *Effective field theories of axion, ALP and dark photon*, *JHEP* **01** (2024) 161, [[2305.16770](#)].

[23] C. Delaunay, T. Kitahara, Y. Soreq and J. Zupan, *Light scalar beyond the Higgs mixing limit*, [2501.16477](#).

[24] C. Englert, G. F. Giudice, A. Greljo and M. McCullough, *The \hat{H} -Parameter: An Oblique Higgs View*, *JHEP* **09** (2019) 041, [[1903.07725](#)].

[25] C. G. Callan, Jr., S. R. Coleman, J. Wess and B. Zumino, *Structure of phenomenological Lagrangians. 2.*, *Phys. Rev.* **177** (1969) 2247–2250.

[26] S. R. Coleman, J. Wess and B. Zumino, *Structure of phenomenological Lagrangians. 1.*, *Phys. Rev.* **177** (1969) 2239–2247.

[27] J. Wess and B. Zumino, *Consequences of anomalous Ward identities*, *Phys. Lett. B* **37** (1971) 95–97.

[28] E. Witten, *Global Aspects of Current Algebra*, *Nucl. Phys. B* **223** (1983) 422–432.

[29] G. Källén, *On the definition of the Renormalization Constants in Quantum Electrodynamics*, *Helv. Phys. Acta* **25** (1952) 417.

[30] H. Lehmann, *On the Properties of propagation functions and renormalization constants of quantized fields*, *Nuovo Cim.* **11** (1954) 342–357.

[31] H. Georgi, *Unparticle physics*, *Phys. Rev. Lett.* **98** (2007) 221601, [[hep-ph/0703260](#)].

[32] N. Arkani-Hamed, M. Porrati and L. Randall, *Holography and phenomenology*, *JHEP* **08** (2001) 017, [[hep-th/0012148](#)].

[33] I. R. Klebanov and E. Witten, *AdS / CFT correspondence and symmetry breaking*, *Nucl. Phys. B* **556** (1999) 89–114, [[hep-th/9905104](#)].

[34] G. Cacciapaglia, G. Marandella and J. Terning, *The AdS/CFT/Unparticle Correspondence*, *JHEP* **02** (2009) 049, [[0804.0424](#)].

[35] P. J. Fox, A. Rajaraman and Y. Shirman, *Bounds on Unparticles from the Higgs Sector*, *Phys. Rev. D* **76** (2007) 075004, [[0705.3092](#)].

[36] G. Cacciapaglia, G. Marandella and J. Terning, *Colored Unparticles*, *JHEP* **01** (2008) 070, [[0708.0005](#)].

[37] E. Witten, *Anti de Sitter space and holography*, *Adv. Theor. Math. Phys.* **2** (1998) 253–291, [[hep-th/9802150](#)].

[38] M. Froissart, *Asymptotic behavior and subtractions in the Mandelstam representation*, *Phys. Rev.* **123** (1961) 1053–1057.

[39] M. Jacob and G. C. Wick, *On the General Theory of Collisions for Particles with Spin*, *Annals Phys.* **7** (1959) 404–428.

[40] L. Di Luzio, J. F. Kamenik and M. Nardecchia, *Implications of perturbative unitarity for scalar di-boson resonance searches at LHC*, *Eur. Phys. J. C* **77** (2017) 30, [[1604.05746](#)].

[41] ATLAS, CMS collaboration, G. Aad et al., *Measurements of the Higgs boson production and decay rates and constraints on its couplings from a combined ATLAS and CMS analysis of the LHC pp collision data at $\sqrt{s} = 7$ and 8 TeV*, *JHEP* **08** (2016) 045, [[1606.02266](#)].

[42] H. Davoudiasl, T. Han and H. E. Logan, *Discovering an invisibly decaying Higgs at hadron colliders*, *Phys. Rev. D* **71** (2005) 115007, [[hep-ph/0412269](#)].

[43] P. J. Fox, R. Harnik, J. Kopp and Y. Tsai, *Missing Energy Signatures of Dark Matter at the LHC*, *Phys. Rev. D* **85** (2012) 056011, [[1109.4398](#)].

[44] C. Englert, J. Jaeckel, E. Re and M. Spannowsky, *Evasive Higgs Maneuvers at the LHC*, *Phys. Rev. D* **85** (2012) 035008, [[1111.1719](#)].

[45] C. Englert, K. Nordström and M. Spannowsky, *Towards resolving strongly-interacting dark sectors at colliders*, *Phys. Rev. D* **94** (2016) 055028, [[1606.05359](#)].

[46] O. J. P. Eboli and D. Zeppenfeld, *Observing an invisible Higgs boson*, *Phys. Lett. B* **495** (2000) 147–154, [[hep-ph/0009158](#)].

[47] ATLAS collaboration, G. Aad et al., *Combination of searches for invisible decays of the Higgs boson using 139 fb $^{-1}$ of proton-proton collision data at $s=13$ TeV collected with the ATLAS experiment*, *Phys. Lett. B* **842** (2023) 137963, [[2301.10731](#)].

[48] C. Englert and M. McCullough, *Modified Higgs Sectors and NLO Associated Production*, *JHEP* **07** (2013) 168, [[1303.1526](#)].

[49] N. Craig, C. Englert and M. McCullough, *New Probe of Naturalness*, *Phys. Rev. Lett.* **111** (2013) 121803, [[1305.5251](#)].

[50] E. Alvarez, D. A. Faroughy, J. F. Kamenik, R. Morales and A. Szynkman, *Four tops for LHC*, *Nucl. Phys. B* **915** (2017) 19–43, [[1611.05032](#)].

[51] L. Darmé, B. Fuks and M. Goodsell, *Cornering sgluons with four-top-quark events*, *Phys. Lett. B* **784** (2018) 223–228, [[1805.10835](#)].

[52] E. Alvarez, A. Juste and R. M. S. Seoane, *Four-top as probe of light top-philic New Physics*, *JHEP* **12** (2019) 080, [[1910.09581](#)].

[53] L. Darmé, B. Fuks and F. Maltoni, *Top-philic heavy resonances in four-top final states and their EFT interpretation*, *JHEP* **09** (2021) 143, [[2104.09512](#)].

[54] F. Blekman, F. Déliot, V. Dutta and E. Usai, *Four-top quark physics at the LHC*, *Universe* **8** (2022) 638, [[2208.04085](#)].

[55] Anisha, O. Atkinson, A. Bhardwaj, C. Englert, W. Naskar and P. Stylianou, *BSM reach of four-top production at the LHC*, *Phys. Rev. D* **108** (2023) 035001, [[2302.08281](#)].

[56] R. Frederix, D. Pagani and M. Zaro, *Large NLO corrections in $t\bar{t}W^\pm$ and $t\bar{t}t\bar{t}$ hadroproduction from supposedly subleading EW contributions*, *JHEP* **02** (2018) 031, [[1711.02116](#)].

[57] N. Kauer and G. Passarino, *Inadequacy of zero-width approximation for a light Higgs boson signal*, *JHEP* **08** (2012) 116, [[1206.4803](#)].

[58] C. Englert and M. Spannowsky, *Limitations and Opportunities of Off-Shell Coupling Measurements*, *Phys. Rev. D* **90** (2014) 053003, [[1405.0285](#)].

[59] S.-P. He and S.-h. Zhu, *One-loop radiative correction to the triple Higgs coupling in the Higgs singlet model*, *Phys. Lett. B* **764** (2017) 31–37, [[1607.04497](#)].

[60] A. Voigt and S. Westhoff, *Virtual signatures of dark sectors in Higgs couplings*, *JHEP* **11** (2017) 009, [[1708.01614](#)].

[61] C. Englert and J. Jaeckel, *Probing the Symmetric Higgs Portal with Di-Higgs Boson Production*, *Phys. Rev. D* **100** (2019) 095017, [[1908.10615](#)].

[62] I. Brivio, O. J. P. Éboli, M. B. Gavela, M. C. Gonzalez-Garcia, L. Merlo and S. Rigolin, *Higgs ultraviolet softening*, *JHEP* **12** (2014) 004, [[1405.5412](#)].

[63] M. J. Herrero and R. A. Morales, *One-loop renormalization of vector boson scattering with the electroweak chiral Lagrangian in covariant gauges*, *Phys. Rev. D* **104** (2021) 075013, [[2107.07890](#)].

[64] Anisha, D. Domenech, C. Englert, M. J. Herrero and R. A. Morales, *Bosonic multi-Higgs correlations beyond leading order*, *Phys. Rev. D* **110** (2024) 095016, [[2405.05385](#)].

[65] G. Passarino and M. J. G. Veltman, *One Loop Corrections for e^+e^- Annihilation Into $\mu^+\mu^-$ in the Weinberg Model*, *Nucl. Phys. B* **160** (1979) 151–207.

[66] C. Englert, T. Ingebretsen Carlson, J. Sjölin and M. Spannowsky, *Harnessing Higgs Kinematics for HEFT Constraints*, [2506.19401](#).

[67] M. Cepeda et al., *Report from Working Group 2: Higgs Physics at the HL-LHC and HE-LHC*, *CERN Yellow Rep. Monogr.* **7** (2019) 221–584, [[1902.00134](#)].

[68] FCC collaboration, *Prospects in electroweak, Higgs and Top physics at FCC*, .

[69] P. Bambade et al., *The International Linear Collider: A Global Project*, [1903.01629](#).

[70] CLICDP, CLIC collaboration, T. K. Charles et al., *The Compact Linear Collider (CLIC) - 2018 Summary Report*, *CERN Yellow Rep. Monogr.* **2** (2018) 1–112, [[1812.06018](#)].

[71] CEPC STUDY GROUP collaboration, W. Abdallah et al., *CEPC Technical Design Report: Accelerator, Radiat. Detect. Technol. Methods* **8** (2024) 1–1105, [[2312.14363](#)].

[72] LINEAR COLLIDER VISION collaboration, D. Attié et al., *A Linear Collider Vision for the Future of Particle Physics*, [2503.19983](#).

[73] LINEAR COLLIDER collaboration, A. Subba et al., *The Linear Collider Facility (LCF) at CERN*, [2503.24049](#).

[74] G. J. van Oldenborgh and J. A. M. Vermaseren, *New Algorithms for One Loop Integrals*, *Z. Phys. C* **46** (1990) 425–438.

[75] R. Mertig, M. Bohm and A. Denner, *FEYN CALC: Computer algebraic calculation of Feynman amplitudes*, *Comput. Phys. Commun.* **64** (1991) 345–359.

[76] T. Hahn, *Generating Feynman diagrams and amplitudes with FeynArts 3*, *Comput. Phys. Commun.* **140** (2001) 418–431, [[hep-ph/0012260](#)].

[77] T. Hahn and M. Perez-Victoria, *Automatized one loop calculations in four-dimensions and D-dimensions*, *Comput. Phys. Commun.* **118** (1999) 153–165, [[hep-ph/9807565](#)].

[78] T. Hahn, *Automatic loop calculations with FeynArts, FormCalc, and LoopTools*, *Nucl. Phys. B Proc. Suppl.* **89** (2000) 231–236, [[hep-ph/0005029](#)].

[79] V. Shtabovenko, R. Mertig and F. Orellana, *New Developments in FeynCalc 9.0*, *Comput. Phys. Commun.* **207** (2016) 432–444, [[1601.01167](#)].

[80] V. Shtabovenko, R. Mertig and F. Orellana, *FeynCalc 9.3: New features and improvements*, *Comput. Phys. Commun.* **256** (2020) 107478, [[2001.04407](#)].

[81] ATLAS collaboration, G. Aad et al., *Observation of four-top-quark production in the multilepton final state with the ATLAS detector*, *Eur. Phys. J. C* **83** (2023) 496, [[2303.15061](#)].

[82] CMS collaboration, A. Tumasyan et al., *First measurement of the top quark pair production cross section in proton-proton collisions at $\sqrt{s} = 13.6$ TeV*, *JHEP* **08** (2023) 204, [[2303.10680](#)].

[83] A. Belvedere, C. Englert, R. Kogler and M. Spannowsky, *Dispelling the $\sqrt{\mathcal{L}}$ myth for the High-Luminosity LHC*, *Eur. Phys. J. C* **84** (2024) 715, [[2402.07985](#)].

[84] J. Alwall, R. Frederix, S. Frixione, V. Hirschi, F. Maltoni, O. Mattelaer et al., *The automated computation of tree-level and next-to-leading order differential cross sections, and their matching to parton shower simulations*, *JHEP* **07** (2014) 079, [[1405.0301](#)].

[85] K. Arnold et al., *VBFNLO: A Parton level Monte Carlo for processes with electroweak bosons*, *Comput. Phys. Commun.* **180** (2009) 1661–1670, [[0811.4559](#)].

[86] A. Denner, *Techniques for calculation of electroweak radiative corrections at the one loop level and results for W physics at LEP-200*, *Fortsch. Phys.* **41** (1993) 307–420, [[0709.1075](#)].

[87] A. Denner and S. Dittmaier, *Electroweak Radiative Corrections for Collider Physics*, *Phys. Rept.* **864** (2020) 1–163, [[1912.06823](#)].

[88] J. M. Campbell, R. K. Ellis and C. Williams, *Bounding the Higgs Width at the LHC Using Full Analytic Results for $gg \rightarrow e^-e^+\mu^-\mu^+$* , *JHEP* **04** (2014) 060, [[1311.3589](#)].

[89] G. Buchalla, O. Cata, A. Celis, M. Knecht and C. Krause, *Complete One-Loop Renormalization of the Higgs-Electroweak Chiral Lagrangian*, *Nucl. Phys. B* **928** (2018) 93–106, [[1710.06412](#)].

[90] CMS collaboration, G. Aad et al., *Highlights of the HL-LHC physics projections by ATLAS and CMS*, [2504.00672](#).

[91] G. Heinrich, J. Lang and L. Scyboz, *SMEFT predictions for $gg \rightarrow hh$ at full NLO QCD and truncation uncertainties*, *JHEP* **08** (2022) 079, [[2204.13045](#)].

[92] E. Bagnaschi, G. Degrassi and R. Gröber, *Higgs boson pair production at NLO in the POWHEG approach and the top quark mass uncertainties*, *Eur. Phys. J. C* **83** (2023) 1054, [[2309.10525](#)].

[93] J. R. Espinosa and M. Quiros, *The Electroweak phase transition with a singlet*, *Phys. Lett. B* **305** (1993) 98–105, [[hep-ph/9301285](#)].

[94] D. Curtin, P. Meade and C.-T. Yu, *Testing Electroweak Baryogenesis with Future Colliders*, *JHEP* **11** (2014) 127, [[1409.0005](#)].

[95] M. Carena, Z. Liu and Y. Wang, *Electroweak phase transition with spontaneous Z_2 -breaking*, *JHEP* **08** (2020) 107, [[1911.10206](#)].

[96] M. J. Ramsey-Musolf, T. V. I. Tenkanen and V. Q. Tran, *Refining Gravitational Wave and Collider Physics Dialogue via Singlet Scalar Extension*, [2409.17554](#).

[97] L. Niemi, M. J. Ramsey-Musolf and G. Xia, *Nonperturbative study of the electroweak phase transition in the real scalar singlet extended standard model*, *Phys. Rev. D* **110** (2024) 115016, [[2405.01191](#)].

[98] P. Basler, L. Biermann, M. Mühlleitner, J. Müller, R. Santos and J. Viana, *BSMPT v3 a tool for phase transitions and primordial gravitational waves in extended Higgs sectors*, *Comput. Phys. Commun.* **316** (2025) 109766, [[2404.19037](#)].

[99] D. Balui, J. Chakrabortty, D. Dey and S. Mohanty, *Gauge invariant effective potential*, *Phys. Rev. D* **111** (2025) 085032, [[2502.17156](#)].

[100] M. Quiros, *Finite temperature field theory and phase transitions*, in *ICTP Summer School in High-Energy Physics and Cosmology*, pp. 187–259, 1, 1999. [hep-ph/9901312](#).

[101] G. Alguero, G. Belanger, F. Boudjema, S. Chakraborti, A. Goudelis, S. Kraml et al., *micrOMEGAs 6.0: N-component dark matter*, *Comput. Phys. Commun.* **299** (2024) 109133, [[2312.14894](#)].

- [102] W. J. G. de Blok, *The Core-Cusp Problem*, *Adv. Astron.* **2010** (2010) 789293, [[0910.3538](#)].
- [103] M. Boylan-Kolchin, J. S. Bullock and M. Kaplinghat, *Too big to fail? The puzzling darkness of massive Milky Way subhaloes*, *Mon. Not. Roy. Astron. Soc.* **415** (2011) L40, [[1103.0007](#)].
- [104] A. A. Klypin, A. V. Kravtsov, O. Valenzuela and F. Prada, *Where are the missing Galactic satellites?*, *Astrophys. J.* **522** (1999) 82–92, [[astro-ph/9901240](#)].
- [105] J. C. Criado and M. Pérez-Victoria, *Field redefinitions in effective theories at higher orders*, *JHEP* **03** (2019) 038, [[1811.09413](#)].
- [106] M. J. Herrero and R. A. Morales, *One-loop corrections for WW to HH in Higgs EFT with the electroweak chiral Lagrangian*, *Phys. Rev. D* **106** (2022) 073008, [[2208.05900](#)].